euspen's 26th International Conference & Exhibition, Krakow, PL, June 2026
www.euspen.eu

Elucidating the effect of wobble frequency on the fluid flow and keyhole dynamics in the laser lap welding of electric vehicles battery packs

Akash Meena[1], Guido Tosello[1]

[1] *Department of Civil and Mechanical Engineering, Technical University of Denmark, 2800 Kgs. Lyngby, Denmark*

akmee@dtu.dk

Abstract The integrity of the laser welding joints at the interface between battery tabs and busbars is crucial for ensuring the safety and efficiency of electric vehicles (EVs). Despite advancements in laser welding techniques, the effect of varying interface position on melt pool morphology, fluid flow, and keyhole stability remains unexplored. This study examined how wobble frequency in a lap-joint laser welding affected fluid flow, melt pool depth and keyhole dynamics in AA1050 aluminum sheets. A ring spot beam introduced to minimize spatter in the melt pool. A combined experimental and numerical methodology was adopted, in which the 150 Hz wobble condition was validated experimentally and additional wobble frequencies were analysed using a CFD-based FLOW-3D model. The results reveal that the different wobble frequency alters heat distribution, melt pool convection patterns, and keyhole stability. A 3D multiphysics simulation of laser wobbling with a ring spot beam was implemented. For the 150 Hz case, the predicted melt-pool depth below the interface (~2000 µm) showed close agreement with the experimental value (~1956 µm), while additional simulations indicated a reduction in penetration with increasing wobble frequency.

Keywords: Multiphysics simulation; laser wobble welding; wobbling frequency; laser beam shaping; lap joints; ring beam profile.

1. Introduction

The connection between the busbar and battery tab is critical in electric vehicle (EV) battery packs, directly influencing overall efficiency, safety, thermal stability, and long-term reliability [1,2]. The joint must provide low electrical resistance while maintaining adequate mechanical integrity under vibration, thermal cycling, and service loads [3–5]. In this context, laser welding has emerged as a highly attractive joining technology due to its high precision, localized energy input, automation compatibility, and high productivity [6–8]. Nevertheless, achieving robust and repeatable joints requires careful selection and optimization of process parameters, because small changes in process stability can lead to defects that significantly degrade joint performance.

A large part of the fundamental understanding of laser welding particularly regarding melt-pool fluid flow and keyhole dynamics has been established using single workpiece configurations [9–12]. While such studies are valuable for isolating physical mechanisms, the lap welding configuration introduces additional complexity that remains less explored. The schematic diagram of laser keyhole welding is shown in **Figure 1**.

Kang et al. [10] further linked keyhole instability to bubble generation via three primary mechanisms that contribute to pore formation.

Li et al. [11] used a validated model to quantify porosity reduction in adjustable ring-mode laser welding of aluminium alloys, showing that a ring beam lowers porosity by mitigating keyhole collapse and stabilising melt-pool flow, thereby limiting pore formation at both the gas-liquid and liquid-solid interfaces.

Laser lap welding is particularly sensitive to keyhole instability, which may cause intermittent keyhole collapse, spatter, and pore entrapment near the interface which is the most critical region for mechanical and electrical performance [13–16]. To improve process robustness and widen the effective seam, beam wobbling is frequently applied.

Wobbling can increase weld width (beneficial for mechanical strength and alignment tolerance) and can modify the melt-pool circulation and keyhole response through controlled redistribution of energy in space and time. However, the wobbling strategy involves multiple coupled parameters such as amplitude, frequency, scanning pattern, and often power modulation and their combined influence needs systematic investigation [17].

Among these parameters, wobble frequency is particularly important because it directly sets the timescale of beam motion relative to the characteristic response times of the melt pool and keyhole. In practical terms, frequency strongly affects the degree of overlap between successive oscillation cycles and thereby governs the stability of the keyhole wall, and the development of flow structures in the molten pool.

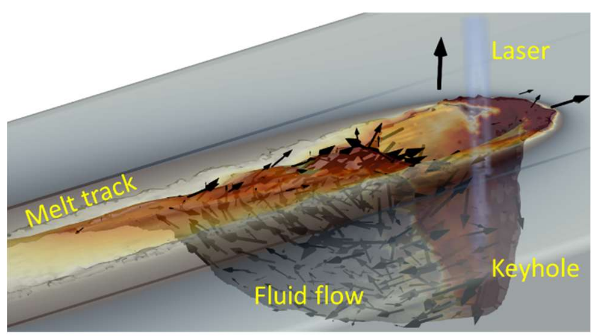

Figure 1. Schematic diagram of laser keyhole welding.

Despite increasing industrial adoption of wobble welding, most laser lap welding studies have emphasized outcomes such as intermetallic compound formation, part-to-part gap effects, segregation behavior or focused on weld-quality trends [18–22].

In contrast, there remains a clear gap in the analysis of fluid flow and keyhole dynamics in laser lap wobble welding. In addition, ring beam shaping has been introduced to mitigate spatter and stabilize the molten pool, further motivating a deeper understanding of the underlying dynamics.

This work aims to elucidate how wobble frequency governs melt-pool flow behaviour and keyhole dynamics, and how these changes translate into weld morphology. The outcomes provide a clearer physical interpretation and support more robust selection of wobble parameters for high-quality laser lap welds in battery interconnect applications.

2. Methodology

This work investigates how wobble frequency influences melt-pool fluid flow and keyhole dynamics during laser lap welding. A controlled experimental work has been conducted by varying wobble frequency (100 Hz, 125 Hz and 150 Hz) while keeping other key processing conditions constant. In parallel, the commercial finite-volume computational fluid dynamics (CFD) solver FLOW-3D (by Flow Science, Inc., Santa Fe, New Mexico, USA) was employed to compute the coupled mass, momentum and energy transport for laser lap wobble welding under different wobble frequencies. The accommodation coefficient (bounded between 0 and 1) was used to represent interfacial phase change behaviour at the free surface, i.e., the fraction of vapour molecules that lose sufficient energy upon impingement to condense into the liquid phase at the vapour-liquid interface. Direct experimental quantification of the evaporation rate is difficult because it is highly sensitive to process conditions (e.g., laser speed, laser power, resulting linear energy density) as well as temperature-dependent material properties. [23,24].

2.1. Experimental design

The experiments were carried out on AA1050 in a lap-joint configuration, using a wobble frequency of 150 Hz. The lap joint consisted of a 1.5 mm upper sheet and a 2.5 mm lower sheet. The applied laser processing parameters are summarized in **Table 1**. A focusing optic with 255 mm focal length and 150 mm collimation length was used, and the laser beam was inclined by approximately 3° to minimize back reflections. X-ray CT scanning was additionally performed to assess the distribution of porosity. All experiments were conducted using a TRUMPF TruDisk 6001 solid-state disk laser equipped with a PFO 33-2 processing head shown in **Figure 2.** The weld length is 15 mm, made using a circular wobbling technique, and the welds were oriented across the sheet width of 25 mm. This modulation was synchronized with the wobble motion to control the laser energy density along the oscillation path. The welding path followed a wobbling pattern generated by a circular laser beam as shown in **Figure 3**. The wobbling amplitude of 1.2 mm and frequency of 150 Hz were selected based on initial parameter screening and are within the relevant range used in industrial practice. Laser power was modulated from 6 kW (100%) to 4.8 kW (80%), and ring beam shaping are shown in

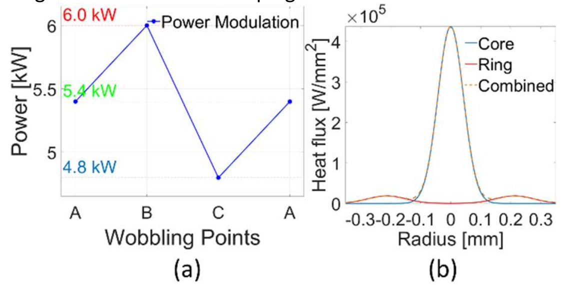

Figure 4.. The core and ring intensities were selected to reproduce the experimental beam-shaping condition and were kept constant in all cases in order to investigate the effect of wobble frequency. All specimens were cleaned with 2-propanol before performing the laser welding experiments. Each experimental condition was repeated twice to ensure reproducibility.

Table 1 Laser welding parameters

Laser parameters	
Power (kW)	6
Power modulation	100-80%
Amplitude (mm)	1.2
Frequency (Hz)	(100, 125, 150) Hz
Feed rate (mm/s)	95, 105, 115, 125
Accomodation coefficient	0.5
Surface tension gradient (N/m/s)	0.00026
Surface tension coefficeint (N/m)	0.871

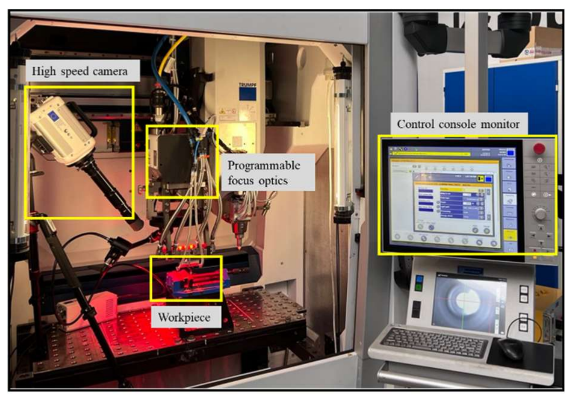

Figure 2. Experimental setup for laser welding experiment.

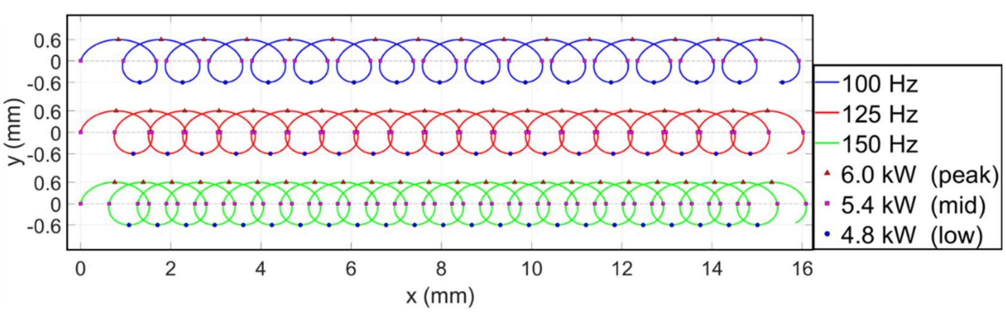

Figure 3. Schematic of laser wobbling path with three different wobble frequency (100 Hz, 120 Hz, 150 Hz).

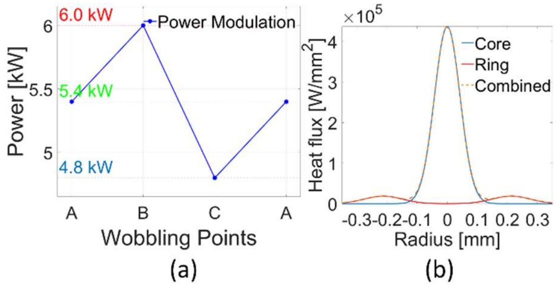

Figure 4. (a) Power modulation during laser wobble welding and (b) Heat flux distribution using the core and ring spot beam used in the laser wobbling process.

2.2. Numerical model

A multi-physics model was implemented in the commercial finite-volume solver FLOW-3D® (v12.0.2.01, release 7 update 3) using the WELD® module, accounting for key mechanisms including recoil pressure, multiple keyhole reflections, a ring-spot beam heat source, and the Marangoni effect.

The main governing equations of mass, linear momentum and energy balance are given by:

$$\nabla \cdot \boldsymbol{u} = \boldsymbol{0} \tag{1}$$

$$\frac{\partial(\rho \boldsymbol{u})}{\partial t} + \rho(\boldsymbol{u} \cdot \nabla)\boldsymbol{u} = -\nabla p + \mu \nabla^2 \boldsymbol{u} - \frac{K_c\left(1 - f_{liq}\right)^2}{C_k + f_{liq}^3}\boldsymbol{u} + F_m \tag{2}$$

$$\rho\left[\frac{\partial h}{\partial t} + (\boldsymbol{u} \cdot \nabla)h\right] = \nabla \cdot (\kappa \nabla T) + \dot{Q}_e \tag{3}$$

In equation (1), **u** ($m \cdot s^{-1}$) represents the velocity vector. In equation (2), ρ ($kg \cdot m^{-3}$) is the fluid density, p (Pa) is the pressure, μ (Pa·s) is the dynamic viscosity and K_c (-) and C_k (-) are two coefficient in Darcy's law to dampen the fluid velocity belonging to the Carman-Kozeny drag force [25], and F_m is the body force that is acting on the liquid/vapour interface. In equation (3), h is the enthalpy (J), κ ($W \cdot (m \cdot K)^{-1}$) is the thermal conductivity, and Q_e (J) is the energy source term.

3. Results

In this section, the melt pool depth is evaluated for different wobbling conditions and the agreement between experimental measurements and numerical predictions is assessed. Figure 5 **(a)** compares the melt pool depth below the interface obtained from the experimental cross-section and the corresponding simulated melt pool profile. Figure 5 **(b)** summarizes the melt pool depth as a function of welding velocity, showing how the penetration changes with travel speed under the same laser and wobbling settings.

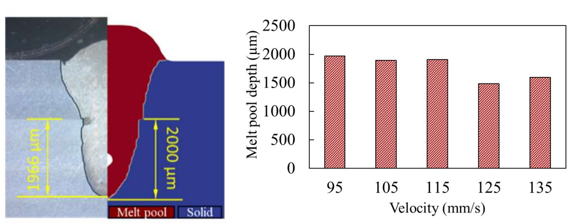

Figure 5. (a) Experimental and numerical comparison at 95 mm/s and (b) and comparison of melt pool height at different feed rate at 150 Hz wobble frequency.

Figure 6 shows that increasing the wobbling frequency reduces the melt pool penetration at the 7.5 mm cross-section. At 100 Hz the melt pool reaches a depth of ~3670 µm, which slightly decreases to ~3600 µm at 125 Hz and drops further to ~3190 µm at 150 Hz.

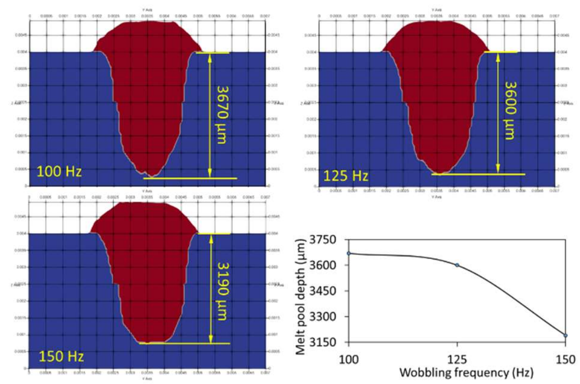

Figure 6. Melt pool depth at 7.5 mm cross-section at 100 Hz, 125 Hz and 150 Hz with 6 kW at 95 mm/s.

This trend indicates that higher wobbling frequencies distribute laser energy over a larger number of oscillation cycles per unit travel length, lowering the local dwell time (and peak heat input) [26]. Hu et al. [27] reported that higher oscillation frequencies required higher laser power to maintain full penetration. This suggests that beam oscillation redistributes the laser energy due to the higher beam velocity along the oscillation path, reducing the local interaction time and effective heat accumulation at a given position. As a result, additional laser power may be required to ensure sufficient penetration.

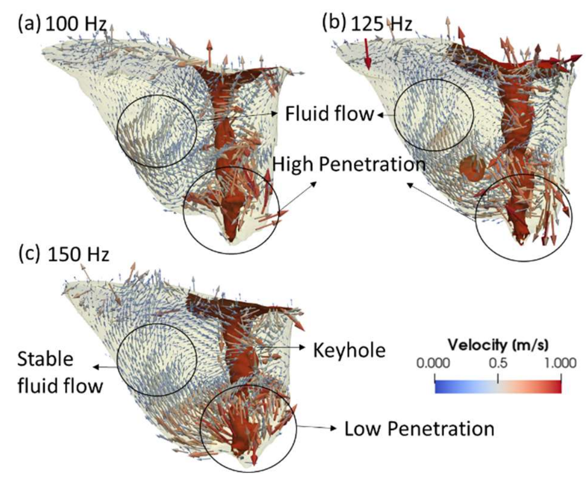

Figure 7. Fluid flow and keyhole depth at (a) 100 Hz, (b) 125 Hz and (c) 150 Hz

Figure 7 illustrates the simulated melt-pool flow field and keyhole morphology at different wobbling frequencies. As the wobbling frequency increases, the keyhole depth gradually decreases, indicating a reduction in penetration. This behaviour can be attributed to the shorter local interaction time of the laser beam at a given position, which reduces the local heat accumulation and limits sustained keyhole development. In addition, the flow field shows a change in the melt-pool dynamics with increasing frequency. At lower frequency, stronger and more irregular recirculating flow patterns with relatively higher local velocities are observed. In contrast, at higher wobbling frequency, the flow appears more uniform and comparatively less intense, suggesting a more stable melt-pool behaviour with reduced fluid velocity. These results indicate that increasing wobbling frequency not only suppresses excessive keyhole growth but also promotes a more stable fluid-flow pattern within the molten pool.

4. Conclusion and Future work

This paper investigated laser lap wobble welding using three wobble frequencies to clarify how wobbling frequency influences melt-pool depth and the resulting weld morphology for battery interconnect applications. Quantitatively, the simulated melt pool depth at a 7.5 mm cross-section decreased with increasing frequency, from ~3670 µm (100 Hz) to ~3600 µm (125 Hz) and ~3190 µm (150 Hz) under identical power and travel speed conditions. A second comparison between experiment and simulation for penetration below the interface showed close agreement, with ~1966 µm (experiment) versus ~2000 µm (numerical), corresponding to an error of ~2%.

From these results, it is demonstrated that wobble frequency is a primary control parameter for penetration in lap wobble welding: increasing frequency (with other parameters fixed) leads to a systematic reduction in melt pool depth, and therefore shallower penetration. This is important because penetration depth directly governs joint formation and robustness in lap welds, and the observed sensitivity means that frequency selection must be treated as a design variable.

Future work will include: (1) extension of the parameter space by varying wobble amplitude and wobble diameter together with frequency to separate geometric spreading effects from frequency effects; (2) carrying out experimental work with all the simulates frequency.

References

[1] P. Stavropoulos, K. Sabatakakis, H. Bikas, Welding Challenges and Quality Assurance in Electric Vehicle Battery Pack Manufacturing, Batteries 2024, Vol. 10, Page 146 10 (2024) 146. https://doi.org/10.3390/BATTERIES10050146.

[2] M.F.R. Zwicker, M. Moghadam, W. Zhang, C. V. Nielsen, Automotive battery pack manufacturing – a review of battery to tab joining, Journal of Advanced Joining Processes 1 (2020) 100017. https://doi.org/10.1016/J.JAJP.2020.100017.

[3] A. Das, D. Li, D. Williams, D. Greenwood, Joining Technologies for Automotive Battery Systems Manufacturing, World Electric Vehicle Journal 2018, Vol. 9, Page 22 9 (2018) 22. https://doi.org/10.3390/WEVJ9020022.

[4] T.I.C. Buidin, F. Mariasiu, Battery Thermal Management Systems: Current Status and Design Approach of Cooling Technologies, Energies 2021, Vol. 14, Page 4879 14 (2021) 4879. https://doi.org/10.3390/EN14164879.

[5] A. Das, A. Barai, I. Masters, D. Williams, Comparison of Tab-To-Busbar Ultrasonic Joints for Electric Vehicle Li-Ion Battery Applications, World Electric Vehicle Journal 2019, Vol. 10, Page 55 10 (2019) 55. https://doi.org/10.3390/WEVJ10030055.

[6] Z. Zhao, S. Janasekaran, G.T. Fong, W. Tayier, J. Zhao, Laser Applications in Ceramic and Metal Joining: A Review, Metals and Materials International 2024 30:7 30 (2024) 1743–1782. https://doi.org/10.1007/s12540-023-01618-0.

[7] M. Dada, P. Popoola, Recent advances in joining technologies of aluminum alloys: a review, Discover Materials 2024 4:1 4 (2024) 86-. https://doi.org/10.1007/s43939-024-00155-w.

[8] R. Nopriantoko, Advancements in Welding Technology: A Comprehensive Review of Techniques, Materials, and Applications, Journal PEP Bandung 2 (2025) 62–110. https://doi.org/10.1234/JM6E4W53.

[9] S. Pang, K. Hirano, R. Fabbro, T. Jiang, Explanation of penetration depth variation during laser welding under variable ambient pressure, J. Laser Appl. 27 (2015) 022007. https://doi.org/10.2351/1.4913455.

[10] S.G. Kang, J. Shin, Numerical and experimental study on melt-pool heat transfer and weld characteristics in dual-mode fiber laser welding of aluminum alloy, Opt. Laser Technol. 158 (2023) 108805. https://doi.org/10.1016/J.OPTLASTEC.2022.108805.

[11] J. Li, P. Jiang, S. Geng, J. Xiong, Numerical and experimental study on keyhole dynamics and pore formation mechanisms during adjustable-ring-mode laser welding of medium-thick aluminum alloy, Int. J. Heat Mass Transf. 214 (2023) 124443. https://doi.org/10.1016/J.IJHEATMASSTRANSFER.2023.124443.

[12] C. Tan, Y. Liu, B. Xu, H. Wang, F. Liu, X. Gong, Z. Zeng, B. Chen, X. Song, Numerical and experimental study of thermal fluid flow and keyhole dynamic in laser welding of aluminum alloy assisted by electromagnetic field, Opt. Laser Technol. 157 (2023) 108718. https://doi.org/10.1016/j.optlastec.2022.108718.

[13] G. Chianese, Q. Hayat, S. Jabar, P. Franciosa, D. Ceglarek, S. Patalano, A multi-physics CFD study to investigate the impact of laser beam shaping on metal mixing and molten pool dynamics during laser welding of copper to steel for battery terminal-to-casing connections, J. Mater. Process. Technol. 322 (2023) 118202. https://doi.org/10.1016/j.jmatprotec.2023.118202.

[14] L. Chen, C. Wang, G. Mi, X. Zhang, Effects of laser oscillating frequency on energy distribution, molten pool morphology and grain structure of AA6061/AA5182 aluminum alloys lap welding, Journal of Materials Research and Technology 15 (2021) 3133–3148. https://doi.org/10.1016/j.jmrt.2021.09.141.

[15] J. Ma, F. Kong, B. Carlson, R. Kovacevic, J. Ma, F. Kong, B. Carlson, R. Kovacevic, Mitigating Zinc Vapor Induced Weld Defects in Laser Welding of Galvanized High-Strength Steel by Using Different Supplementary Means, Welding Processes (2012). https://doi.org/10.5772/53562.

[16] W. Meng, Z. Li, J. Huang, Y. Wu, J. Chen, S. Katayama, The influence of various factors on the geometric profile of laser lap welded T-joints, The International Journal of Advanced Manufacturing Technology 2014 74:9 74 (2014) 1625–1636. https://doi.org/10.1007/s00170-014-6114-y.

[17] S. Sanati, S.F. Nabavi, R. Esmaili, A. Farshidianfar, H. Dalir, A Comprehensive Review of Laser Wobble Welding Processes in Metal Materials: Processing Parameters and Practical Applications, Lasers in Manufacturing and Materials Processing 2024 11:2 11 (2024) 492–528. https://doi.org/10.1007/s40516-024-00245-w.

[18] E.C. Ozkat, P. Franciosa, D. Ceglarek, Development of decoupled multi-physics simulation for laser lap welding considering part-to-part gap, J. Laser Appl. 29 (2017). https://doi.org/10.2351/1.4983234.

[19] R. Oh, D.Y. Kim, D. Ceglarek, The Effects of Laser Welding Direction on Joint Quality for Non-Uniform Part-to-Part Gaps, Metals 2016, Vol. 6, Page 184 6 (2016) 184. https://doi.org/10.3390/met6080184.

[20] D. Basile, R. Al Botros, M. De Maddis, V. Razza, P. Franciosa, Monitoring part-to-part gap and laser power effects in remote laser welding of 1050 aluminum busbar-to-terminal connections via optical microphone sensing, Opt. Laser Technol. 192 (2025) 113494. https://doi.org/10.1016/j.optlastec.2025.113494.

[21] G. Chianese, S. Jabar, P. Franciosa, D. Ceglarek, S. Patalano, A multi-physics CFD study on the part-to-part gap during remote laser welding of copper-to-steel battery tab connectors with beam wobbling, Procedia CIRP 111 (2022) 484–489. https://doi.org/10.1016/J.PROCIR.2022.08.075.

[22] H.-K. Kim, Effects of part-to-part gap and the direction of welding on laser welding quality, (n.d.). https://scholarworks.unist.ac.kr/bitstream/201301/82863/2/000001696715.pdf

[23] S.C.K. De Schepper, G.J. Heynderickx, G.B. Marin, Modeling the evaporation of a hydrocarbon feedstock in the convection section of a steam cracker, Comput. Chem. Eng. 33 (2009) 122–132. https://doi.org/10.1016/J.COMPCHEMENG.2008.07.013.

[24] F. Municchi, H.R. Moran, I. El Mellas, O.K. Matar, M. Magnini, DIRECT NUMERICAL SIMULATIONS OF FLOW BOILING IN MICROCHANNELS, (2022) 4–6.

[25] V.R. Voller, C. Prakash, A fixed grid numerical modelling methodology for convection-diffusion mushy region phase-change problems, Int. J. Heat Mass Transf. 30 (1987) 1709–1719. https://doi.org/10.1016/0017-9310(87)90317-6.

[26] L. Chen, C. Wang, G. Mi, X. Zhang, Effects of laser oscillating frequency on energy distribution, molten pool morphology and grain structure of AA6061/AA5182 aluminum alloys lap welding, Journal of Materials Research and Technology 15 (2021) 3133–3148. https://doi.org/10.1016/j.jmrt.2021.09.141.

[27] K. Hu, W. Muneer, J. Zhang, X. Zhan, Effect of beam oscillating frequency on the microstructure and mechanical properties of dissimilar laser welding of AA2060 and AA6061 alloy, Materials Science and Engineering: A 832 (2022). https://doi.org/10.1016/j.msea.2021.142431.